Wellbore Plastering during CasingwhileDrilling Prediction

by

Chew Jay Sern

12545

Dissertation submitted in partial fulfillment of
the requirement for the
Bachelor of Engineering (Hons)
(Mechanical Engineering)

September 2013

UniversitiTeknologi PETRONAS
Bandar Seri Iskandar
31750 Tronoh
Perak DarulRidzuan

CERTIFICATION OF APPROVAL

Wellbore Plastering during Casing while Drilling Prediction

by

Chew Jay Sern

A project dissertation submitted to the
Mechanical Engineering Programme
UniversitiTeknologi PETRONAS
in partial fulfilment of the requirement for the
BACHELOR OF ENGINEERING (Hons)
(MECHANICAL ENGINEERING)

Approved by,

_____

(Dr. William Pao)

UNIVERSITI TEKNOLOGI PETRONAS

TRONOH, PERAK

August 2013

CERTIFICATION OF ORIGINALITY

This is to certify that I am responsible for the work submitted in this project, that the original work is my own except as specified in the references and acknowledgements, and that the original work contained herein have not been undertaken or done by unspecified sources or persons.

_____

CHEW JAY SERN

ABSTRACT

Wellbore plastering is a phenomenon where mud cake is formed around the wall of wellbore due to cutting plastering to the borehole wall during CasingwhileDrilling (CwD). Wellbore plastering effect can enhance wellbore stability and reduce lost circulation. Predicting the factors that will affect the formation of mud cake is a major challenge because there are many variables, which affect the thickness of mud cake during CwD. The objective of this study is to investigate the factors that affect the thickness of mud cake formed on the borehole wall at different operating conditions. Furthermore, the objective of this study is scoped down to two operating factors, namely casing rotational speed and annular velocity. The study is started with the formation of three dimensional multiphase fluid simulation model, followed by parametric study on the two operating factors using ANSYS Fluent. The result of this study has shown the correlation of thickness of mud cake formed and casing rotational speed and annular velocity.

Keywords-Mud Cake, Plastering Effect, Simulation, Fluent

TABLE OF CONTENTS

LIST OF FIGURES

LIST OF TABLES

CHAPTER 1 INTRODUCTION

1.1 Project Background

Casing while Drilling (CwD) is a process where casing and drilling are carried out simultaneously while the casing is rotated as needed to drill. Unlike CwD, conventional drilling is done where casing process is done separately after drilling. The annulus space between open hole and casing of CwD is larger than that of conventional drilling. CwD has been demonstated to reduce lost circulation and improve wellbore strength.

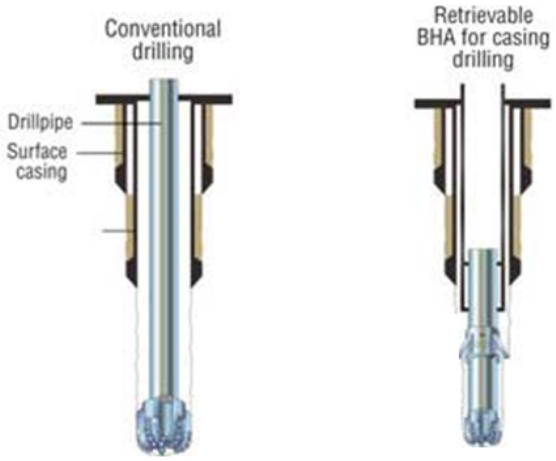

Figure 1.1 Conventional Drilling and Casing Drilling (Mohammed *et al,* 2012)

Wellbore plastering happens during CwD and it is also known as smear effect. This is a phenomenon of the formation of mud cake around the wall of wellbore due to cutting plastering to the borehole wall. The advantages of wellbore plastering are to provide wellbore stability and reduce lost circulation.

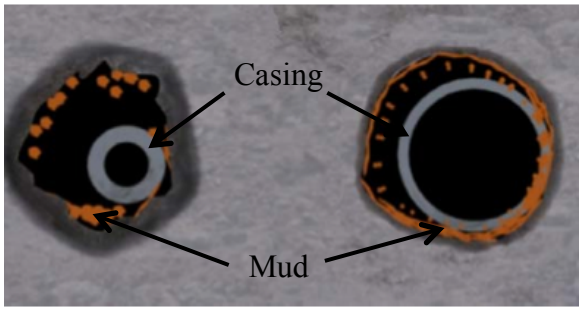

Figure 1.2 Wellbore Stability Improvement by Casing Drilling as Compared to Conventional Drilling (Moellendick *et al*, 2011)

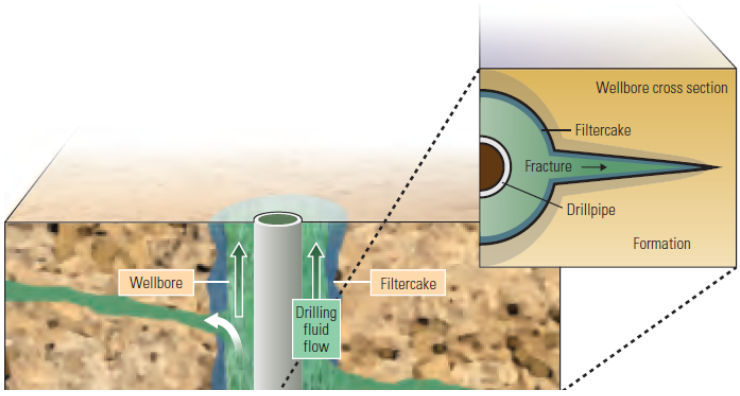

Figure 1.3 Mechanism of Drilling Fluid Egress from the Wellbore (Cook et al, 2012)

The mechanism of wellbore plastering is shown in Figure 1.3. During circulation of drilling mud back to the surface (green arrows), the fluid comes into contact with the wellbore. In conventional drilling practices, the pressure in the wellbore exceeds that of the formation, which prevents formation fluids from entering the wellbore. In one method of fluid loss from the wellbore, a filtration process takes place in the permeable rock, whereby the liquid component of the drilling mud moves into the rock, leaving the solid particulates and emulsion droplets to collect on the wellbore wall and form a layer of mud cake.

1.2 Problem Statement

In wellbore plastering, there are two important factors that affect the thickness of mud cake formed on the borehole wall, namely casing rotational speed, and annular velocity.

One of the key issues is the unclear idea of which factors that will lead to a uniform layer of mud cake formed on the borehole wall. There has been a lack of studies on the correlation between the two important factors and thickness of mud cake formed.

1.3 Objectives

The research objectives can be summarized as follows:

a) To develop a three dimensional multi-phase fluid flow model for wellbore plastering using CFD.
b) To investigate on how the two important operating factors that will affect the thickness of mud cake formed on the borehole wall at different conditions using ANSYS Fluent.

1.4 Scope of Study

For this study, the main focus is to investigate the operating factors that will affect the thickness of mud cake formed during wellbore plastering. Among the operating factors that will be tested are casing rotational speed and annular velocity.

CHAPTER 2 LITERATURE REVIEW

2.1 CasingwhileDrilling (CwD)

Moellendick *et al* (2011) mentioned that CasingwhileDrilling (CwD) is a process in which a well is drilled and cased simultaneously. The advantages of casing while drilling are elimination of Non Productive Time (NPT), efficient borehole cleaning and plastering effect. Wellbore stability improvement is perhaps the most important of these advantages and is the primary driver for selecting intervals where applying Casing Drilling can be most beneficial. Wellbore stability can be achieved from plastering effect. The significant difference of CwD from conventional drilling is that annulus is smaller in CwD in comparison to conventional drilling.

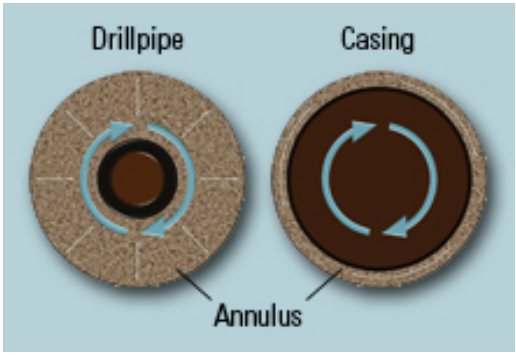

Figure 2.1 The Annulus is Smaller i Casing Drilling in Comparison to Conventional Drilling (Moellendick, 2011)

2.2 Plastering Effect

Salehi *et al* (2013) stated that smooth, continuous contact of the casing during CwD as it rotates against the wellbore wall is the mechanism that results in the plastering effect. Plastering effect also known as smear effect happens when drilled cuttings are packed into any near wellbore fractures and push the filter cake, causing it to build up to an impermeable layer onto the wall of wellbore. The plastering of cuttings to the wellbore wall may enhance wellbore hoop stress by wedging created fractures or increase fracture propagation pressure.

$$P_{frac} = (\lambda + 1)S_h - \lambda p_p \quad (2.1)$$

where

P_{frac} =Fracture propagation pressure ,

λ =Sealing efficiency factor (0-1.5),

S_h =Minimum horizontal stress,

p_p =Pore pressure.

Karimi *et al* (2011) and Moellendick *et al* (2011) stated that plastering effect strengthens the wellbore, prevents lost circulation, enhances continuous drilling, reduces the risk of casing getting stuck during the casing drilling and mitigates formation damage. Kumar *et al* (2013) mentioned that plastering effect mechanism increases the wellbore stability by increasing the fracture gradient of formation. Plastering effect is shown in Figure 2.2.

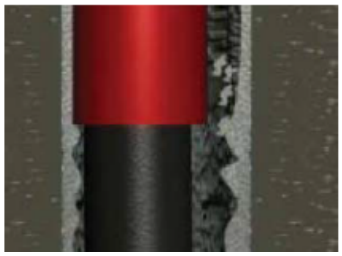

Figure 2.2-A: Casing is forced against the bore wall as it advances into the borehole.

Figure 2.2-B: As mud is smeared into the formation, filter cake builds up on the borehole wall.

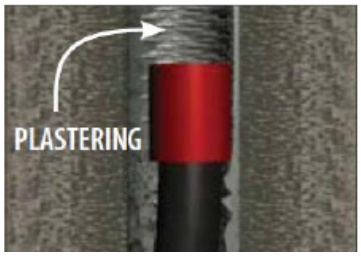

Figure 2.2-A: Filter cake and cuttings are plastered against the borehole wall, sealing porous formations.

Figure 2.2 Plastering Effect (Karimi *et al*, 2011)

2.3 Factors that Affect Plastering Effect

Fontenot *et al* (2004) were the first to study plastering effect. According to their study, improved wellbore stability has been attributed, in part, to the plastering effect achieved when the cuttings and filter cake are pressed into the wall by the combined forces of high annular velocity and pipe rotation; as a result, a highly effective seal is formed, helping to minimize losses. From Fontenot's research, it was found that finer-sized cuttings generated by casing drilling may contribute to the

bridging of cuttings at the porous interface of formation. There are few factors that thought to affect the thickness of mud cake during plastering effect which are casing rotational speed, particle size of cutting, fluid velocity and density of drilling fluid.

2.3.1 Casing Rotational Speed

Salehi et al (2013) stated that the results obtained indicate that casing rotations up to 100 rpm cannot result in mud cake failure. Results for 120 rpm casing rotation indicate that the von Mises stress has exceeded the yield stress of the mud cake, suggesting that increasing the casing rotation over 100 rpm may result in mud cake failure; however, this does not necessarily mean that the mud cake will detach. Having an elastic-plastic mud cake will help to prevent the mud cake detachment from the wellbore wall.

2.3.2 Particle Size of Cutting

Kabir et al (2011) stated that a parametric study on the effects of drilling fluid particle size that was being carried out clearly shows that larger particles form thicker filter cake compared to smaller particles. Larger particles tend to clog the pores of the porous rock formation while small particles penetrate through the porous rock formation. Hence, it is recommended to use larger particle size in drilling fluids to promote the formation of filter cake, which leads to the prevention of drilling fluid loss through the formation.

2.3.3 Ratio of Casing to Annulus Size

Besides, according to Salehi *et al (*2013), ratio of casing to annulus is essential to the occurrence of plastering effect. Small clearance will provide more contact between the casing and mud cake. The effect of casing contact and the forces at contact point can be determined from the mathematical model below. When radial displacement (u) exceeds the clearance (γ), the casing contacts the mud cake. A higher casing size to annulus ratio will decrease the casing displacement during rotation, which subsequently will decrease the contact forces between the casing and the mud cake. The model also shows that both casing size and angular rotation should be designed properly, to avoid deep penetration of the casing into the mud cake.

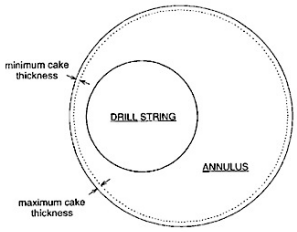

Figure 2.3 Cross Section of Eccentric Annulus Showing Mud Cake Growth (Fisher *et al*, 2000)

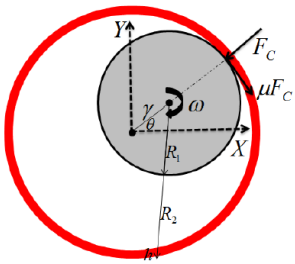

Figure 2.4 Graphical Sketch of Casing Mud Cake Contact (Salehi *et al,*2013)

$$V_{\theta\theta} = R_1\omega + (x\frac{dy}{dt} - y\frac{dx}{dt})/\sqrt{(\frac{x}{y})^2} \quad (2.2)$$

The forces at the contact point:

$$f_x = EI(1 - \frac{\gamma}{u})(x - \mu y sin(V_{\theta\theta})) \quad (2.3)$$

$$f_y = EI(1 - \frac{\gamma}{u})(y - \mu x sin(V_{\theta\theta})) \quad (2.4)$$

$$u = \sqrt{(x^2 + y^2)} \quad (2.5)$$

where

$V_{\theta\theta}$=Tangential velocity at the contact point; h= Mud cake thickness; R_1= Radius of wellbore; R_2= Radius of casing; ω= Casing rotation; γ=Initial clearance of casing from wellbore; EI=Stiffness of casing; μ=Friction coefficient; θ=Inclination angle between the direction radius of the contact point on the X-axis; u=radial displacement of the casing.

Mokhtari *et al* (2012) stated that the impact of plastering effect is more pronounced at higher power-law indexes and higher radius ratios. Small annular space in the casing drilling operations generates significant annular pressures.

Salehi et al (2013) stated that hydraulic results show that a sharp increase in bottom-hole pressure was observed when the casing to hole size ratio exceeded 0.8. This changed the overall equivalent circulating density, which then had to be controlled carefully by optimizing the flow rate in the casing drilling operations. Therefore, ratio of casing to annulus size can be carried out at 0.8.

2.3.4 Annular Velocity

Mokhtari *et al* (2012) stated that lower flow rate reduces the annular pressure loss that could threaten the formation fracture gradient. Moreover, high flow rate can lead to erosion and eventual hole wash out. If the cuttings can be transported effectively with the velocity profile in the conventional drilling, it is possible to reduce the flow rate in casing drilling to accomplish similar velocity profiles. The smaller cutting size and volume as a result of smearing effect also improves the cutting transport. Accordingly, lower flow rate for CwD is recommended due to lower flow rate also reduces annular pressure loss.

2.4 Fluid Flow Model

Bilgesu *et al* (2002) studied cutting transport parameters in both vertical and horizontal wellbores using CFD. The CFD model was used for cuttings and drilling fluids for an incompressible solid-liquid flow with Power Law model. The cutting transport was strongly affected by the cutting size, density and mud circulation rate. In the study, 19 several CFD model runs were carried out with varying drilling fluid densities, casing drillpipe annuli, annular velocities, and particle sizes. It was concluded that, mud weight, viscosity, and flow rate had significant effect on cutting transport.

Mishra *et al* (2007) used CFD simulations to investigate hole cleaning parameters such as flow rate, cutting size, rate of penetration(ROP), drill pipe rotation and inclination angle in directional and horizontal drilling. The research was carried out using water as the transportation fluid. The parameters were graphically analyzed and the calculation of intricate multiphase model was conducted using the Eulerian model. Iterations of runs were conducted at steady state using the

Newtonian fluid. It was observed that the more the fluid velocity increased, the cutting concentration decreased. Drillpipe rotation affects cutting transport of all sizes but small size particles can notably be easily conveyed by the rotation. It was also reported that more cuttings were cleaned as a result of increase in the angle of direction.

These assumptions lead to the following governing equations, which describe the conservation of mass and momentum for both the fluid phase (drilling fluid) and the solid phase (cutting particles):

Mass conservation for liquid phase

$$\frac{\partial \varepsilon}{\partial t} + \frac{\partial}{\partial z}(\varepsilon w_f) = 0 \tag{2.6}$$

Mass conservation for solid phase

$$\frac{\partial \phi}{\partial t} + \frac{\partial}{\partial z}(\varepsilon w_s) = 0 \tag{2.7}$$

Conservation of momentum for the fluid phase

$$\frac{\partial}{\partial t}(\varepsilon w_f) + \frac{\partial}{\partial z}(\varepsilon w_f w_f) = -\frac{\varepsilon}{\overline{\rho_f}}\frac{\partial \rho_f}{\partial z} - (\varepsilon g) + \frac{\beta}{\overline{\rho_f}}(w_f - w_s) \tag{2.8}$$

Conservation of momentum for the solid phase

$$\frac{\partial}{\partial t}(\phi w_s) + \frac{\partial}{\partial z}(\phi w_s w_s) = -\frac{\phi}{\overline{\rho_s}}\frac{\partial \rho_s}{\partial z} - \frac{p_{k,z}}{\overline{\rho_s}}\frac{\partial \phi}{\partial z} - (\phi g) - \frac{\beta}{\overline{\rho_s}}(w_f - w_s) \tag{2.9}$$

where

p_f = fluid phase pressure; p_k = kinematic pressure along the radial direction; p_s = solid phase pressure; t = time; w_f = fluid phase velocity along the axial direction; w_s = solid phase velocity along the axial direction; β = interphase interaction coefficient along the radial direction; ε = fluid phase concentration measured in terms of volume fraction; ϕ = solid phase concentration measured in terms of volume fraction; $\overline{\rho_f}$ = fluid phase material density; $\overline{\rho_s}$ = material density.

2.5 Concluding Remarks

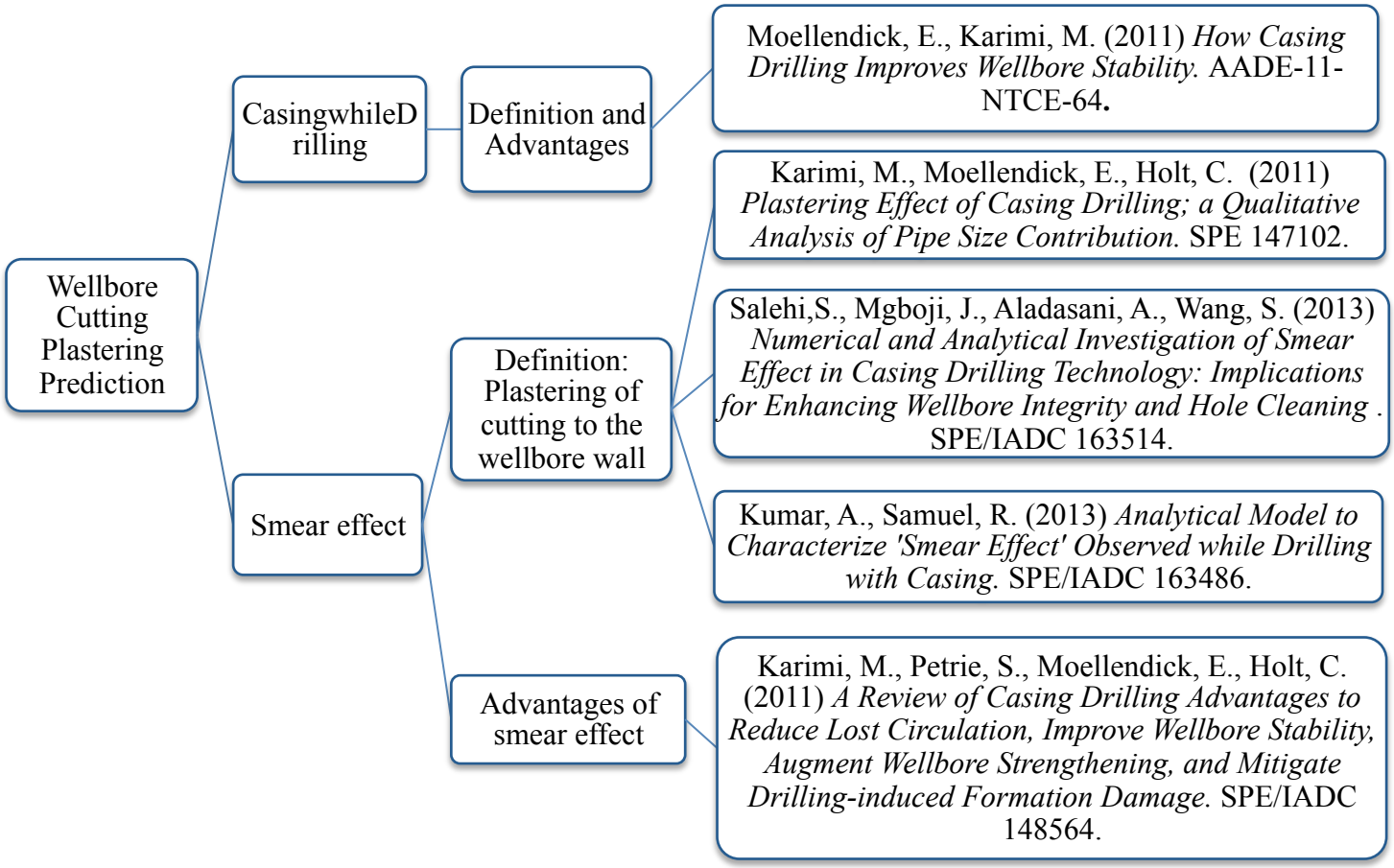

Figure 2.5 Plastering Prediction Concluding Remarks

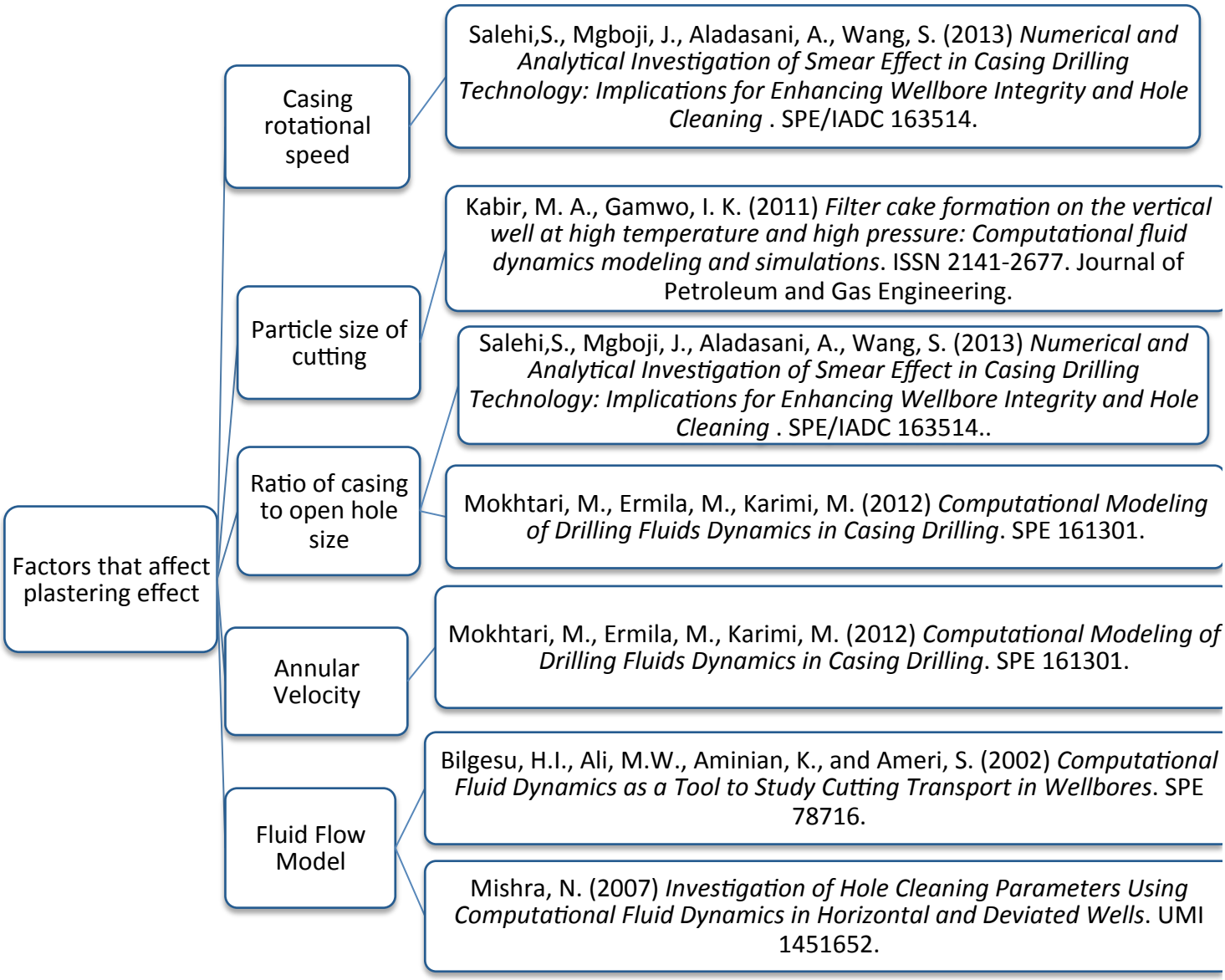

Figure 2.6 Factors that Affect Plastering Effect Concluding Remarks

CHAPTER 3 METHODOLOGY

3.1 Project Process Flow

Figure 3.1 shows the critical phases of the whole research. The project is divided into five phases.

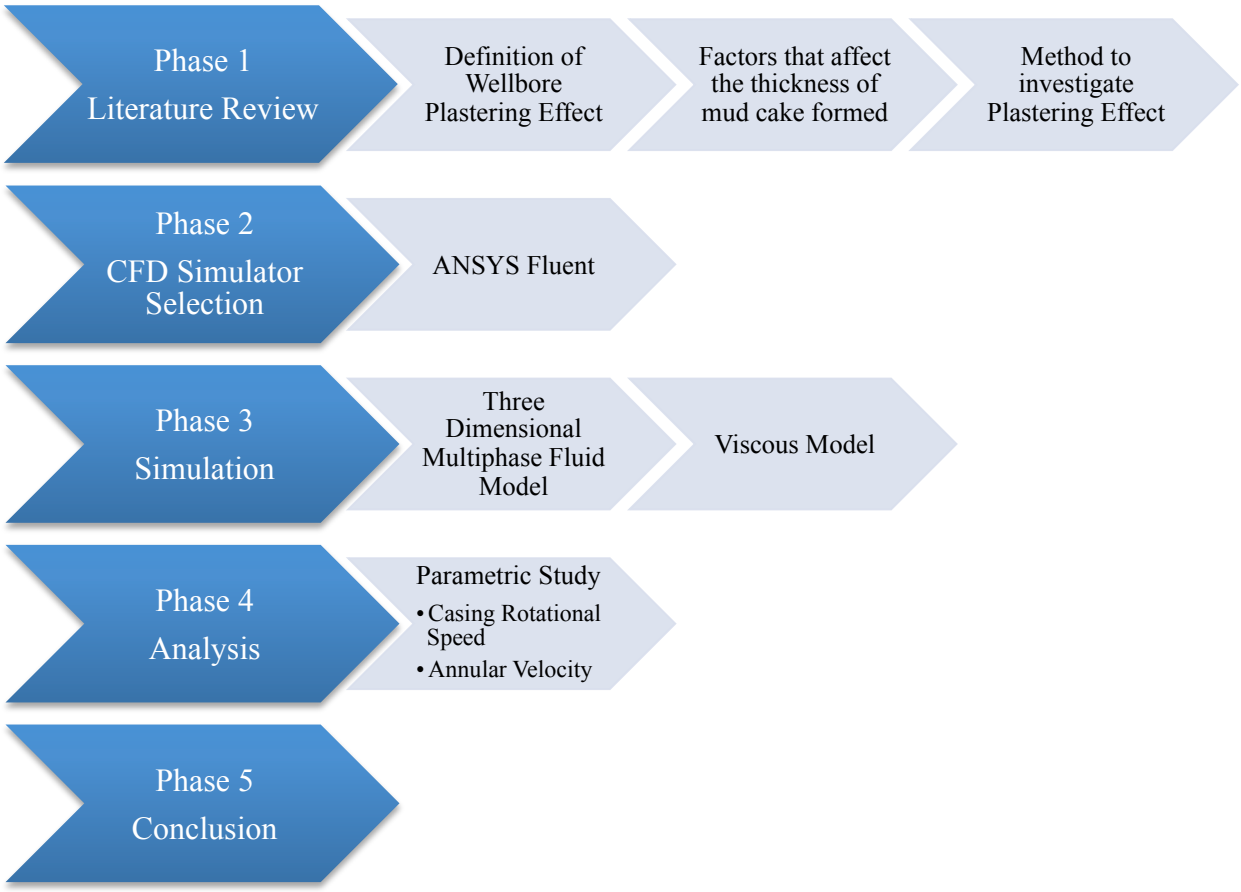

Figure 3.1 Project Process Flow Chart

3.2 ANSYS Fluent Simulation

3.2.1 Multiphase Flow Models

In this study, multiphase model will be considered as there are two or fluids coexist. Mixture model with the materials of non-Newtonian drilling fluid and cuttings is being programmed. As a viscous model, the k-epsilon turbulence model was used. Eulerian multiphase fluid model is chosen in this study.

3.2.2 Boundary Types

Boundary types in Fluent can be classified as follows:

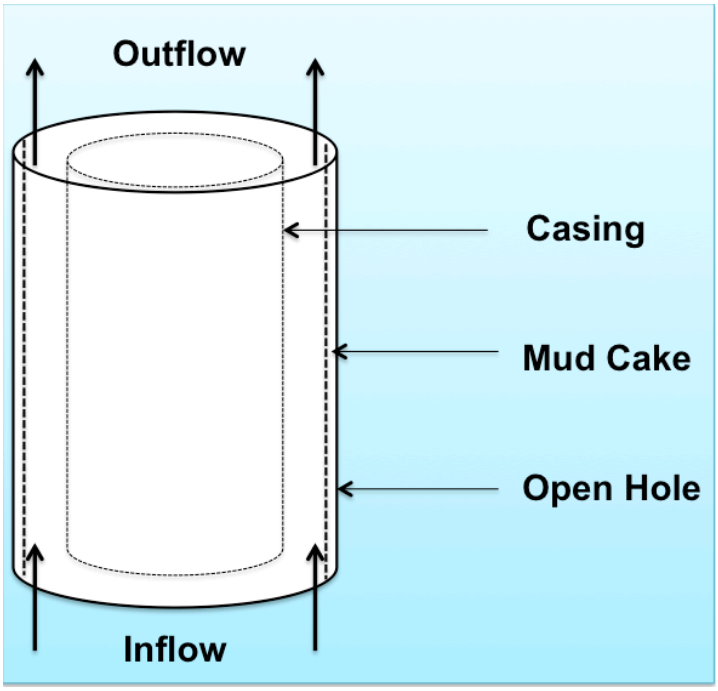

Figure 3.2 Schematic Diagram of Drilling Fluid in the Drilling Zone

The simulation model is constructed with fluid is flowing along the annulus of the wellbore with inflow pressure of 100 kPa and outflow pressure of 0 kPa. As particulate-laden drilling fluid flows upward to the surface through the annulus in between the walls of the wellbore and the casing, differential pressure causes mud cake to build up on the porous rock surface as shown in Figure 4.1. In this CFD simulation, drilling fluid is treated as multiphase non-Newtonian fluid, where solid particulates are suspended in a non- Newtonian fluid phase; the non-Newtonian phase was modeled with power law. The diameter ratio is fixed at 0.8 with outer diameter of 10 inches and inner diameter of 8 inches (Gamwo *et al*, 2011).

3.3 Gantt Charts and Milestones

No	Description	1	2	3	4	5	6	7	8	9	10	11	12	13	14
1	Topic selection	X													
2	Literature Survey		X	X											
3	Familiarizing with simulation program			X	X	X									
4	Defense report preparation					X	♦								
5	Proposal defense presentation						X	♦							
6	Continuation with project - Modeling							X	X	X	X	X	X		
7	Interim report preparation and submission											X	X	X	♦

♦= Key milestone

Table 1 Gantt Chart and Key Milestone for FYP 1

No.	Description	1	2	3	4	5	6	7	8	9	10	11	12	13	14
1	Continuation with project - Modeling and data collecting	X	X	X	X	X	X	X	X						
2	Progress report preparation				X	X	X	X	♦						

	and submission														
3	Continuation with project - Modeling and data collecting									X	X	X	X		
4	Results analyzing -discussion and conclusion									X	X	X	♦		
5	Pre SEDEX											X			
6	Final report preparation									X	X	X	X	♦	
7	Technical paper submission													♦	
8	Final report submission and oral presentation														♦

♦= Key milestone

Table 2 Gantt Chart and Key Milestone for FYP 2

CHAPTER 4 RESULT AND DISCUSSION

4.1 Viscous Model

Turbulence of fluid in this CFD simulation is determined by using Metzner-Reed Reynolds number (Metzner & Reed, 1955). This equation is applied to steady-state flow of non-Newtonian liquids. In this study, non-Newtonian drilling fluid with K of 0.3 and N of 0.51 is considered. Based on the equation 4.1, calculated Reynolds number is 3311 and k-epsilon turbulence model is considered:

$$N_{\mathrm{Re}} = \frac{D_h^n V^{2-n} \rho_f}{K 8^{n-1} \left(\frac{3n+1}{4n} \right)^n} \tag{4.1}$$

<2100 Laminar

>2100 Turbulent

Where:

N_{Re} = Reynolds number; D_h = $D_o - D_i$ (m); V = Inlet velocity (m/s); ρ_f = Fluid density (kg/m^3); K = 0.3; N = 0.51

4.2 Fluid Model

Eulerian multiphase fluid model is considered. Eulerian multiphase model allows for the modeling of multiple separate, yet interacting phases. The phases considered in this study are liquid and solid. In this study, cutting particles, which is secondary phase, is flowing in non-Newtonian drilling fluid, primary phase.

4.3 Meshing

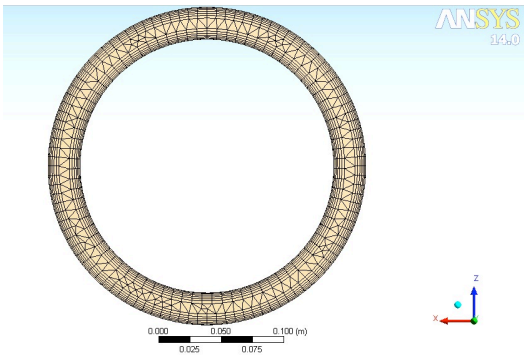

Figure 4.1 Meshing

	Number
Nodes	151353
Elements	321738
Inflation Layer	5

Table 3 Meshing Properties

4.4 Contour of Cutting Volume Fraction

4.4.1 Mud Cake Formation

CFD simulations were performed to simulate mud cake formation in the radial direction on vertical well walls during drilling operations. The differential pressure in the annulus forced the fluid phase through the porous media formation and deposited solid particles in the form of mud cake on the rock surface (open hole), as shown in Figure 4.2 and Figure 4.3. The cutting particles are assumed to be spherical shape of 1mm in diameter with density of 2350 kg/m^3. Initial volume fraction of the cutting is 12.8% as shown in Table 4.

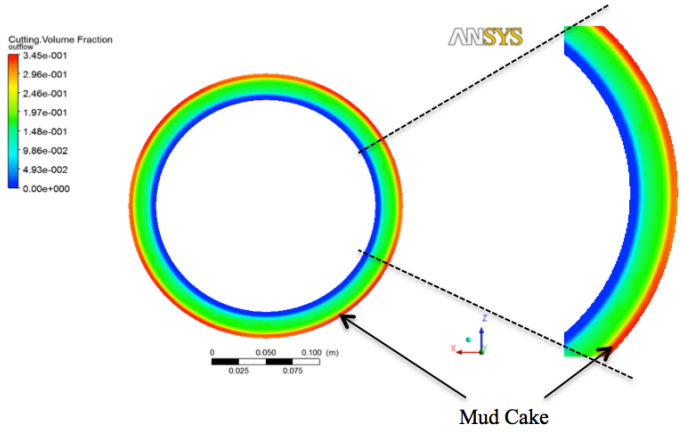

Figure 4.2 Top View of Mud Cake on Wellbore Wall (Cutting Volume Fraction)

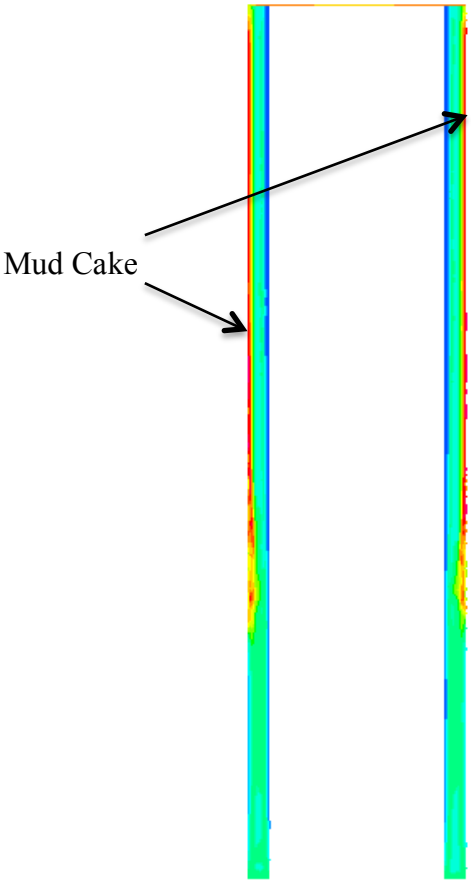

Figure 4.3 Front view of Mud Cake on Wellbore Wall (Cutting Volume Fraction)

	Water	**Cutting**
Volume Fraction	0.815	0.185
Diameter, m	-	0.001
Density, kg/m^3	1000	2350

Viscosity, $kg/m \bullet s$	0.001	0.001

Table 4 Fluid Properties (Gamwo *et al, 2011)*

As the pressure difference between the wellbore and the formation forces the mud cake to consolidate, the fluid phase (cutting) invades the formation. The solid particles become more tightly packed, reducing the permeability of the growing mud cake.

4.4.2 Parametric Study

In this study, investigation on the effect of fluid velocity and casing rotational speed on the thickness of mud cake formed is carried out. Comparison of Figure 4.4 to Figure 4.18 indicates the effect of annular velocity and casing rotational speed on volume fraction of cutting along the wall of openhole. Annular velocity is tested at 0.5m/s, 1.0m/s, 1.5m/s whereas casing rotational speed is tested at 0rpm, 60rpm, 100rpm, 200rpm and 300rpm.

4.4.2.1 Annular Velocity: 0.5m/s

Case 1: 300 rpm Casing Rotational Speed

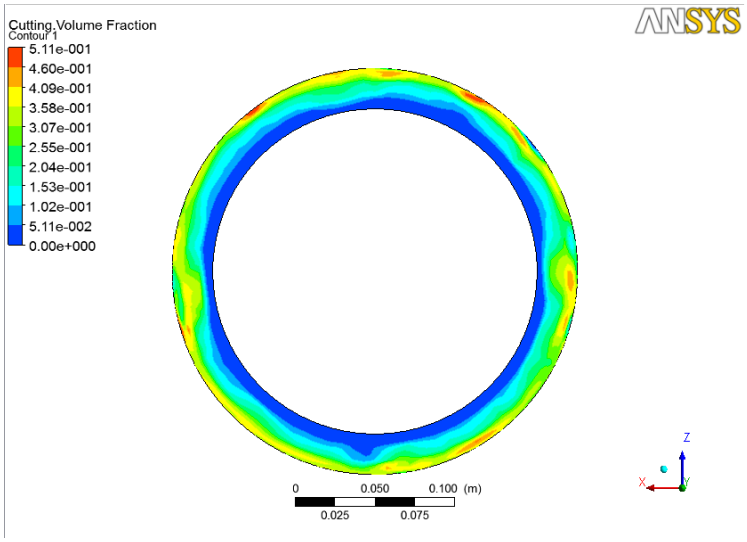

Figure 4.4 Volume Fraction of Cutting (300rpm Casing Rotational Speed)

Case 2: 200 rpm Casing Rotational Speed

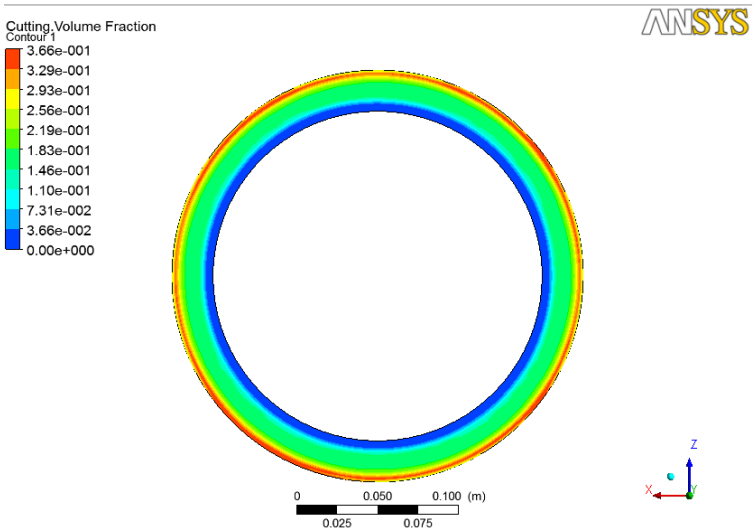

Figure 4.5 Volume Fraction of Cutting (200rpm Casing Rotational Speed)

Case 3: 100 rpm Casing Rotational Speed

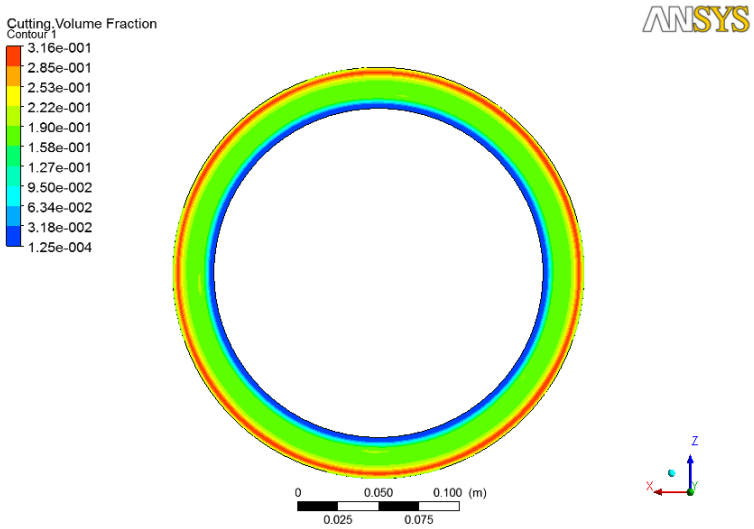

Figure 4.6 Volume Fraction of Cutting (100rpm Casing Rotational Speed)

Case 4: 60 rpm Casing Rotational Speed

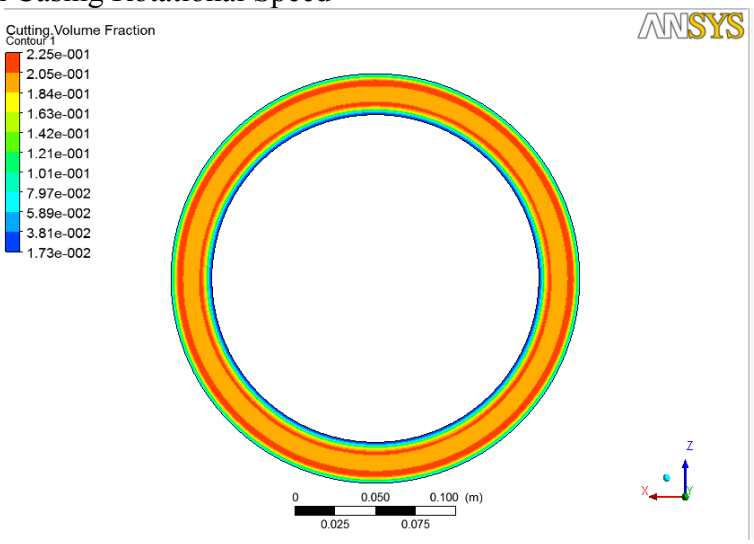

Figure 4.7 Volume Fraction of Cutting (60rpm Casing Rotational Speed)

Case 5: 0 rpm Casing Rotational Speed

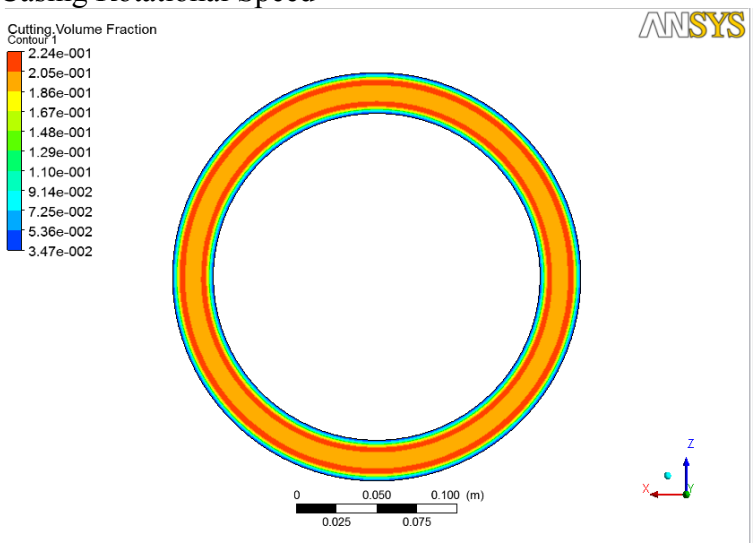

Figure 4.8 Volume Fraction of Cutting (0rpm Casing Rotational Speed)

Figure 4.4 to figure 4.8 show the contours of cutting volume fraction under different casing rotational speed conditions with same cutting particle size of 0.001m, annular velocity of 0.5 m/s and diameter ratio of 0.8. Figure 4.6 shows a nearly uniform distribution of cutting onto the wall of open hole under the condition of 100rpm casing rotational speed. However, non-uniform mud cake is formed when the casing rotational speed is increased up to 300rpm.

4.4.2.2 Annular Velocity: 1.0m/s

Case 6: 300 rpm Casing Rotational Speed

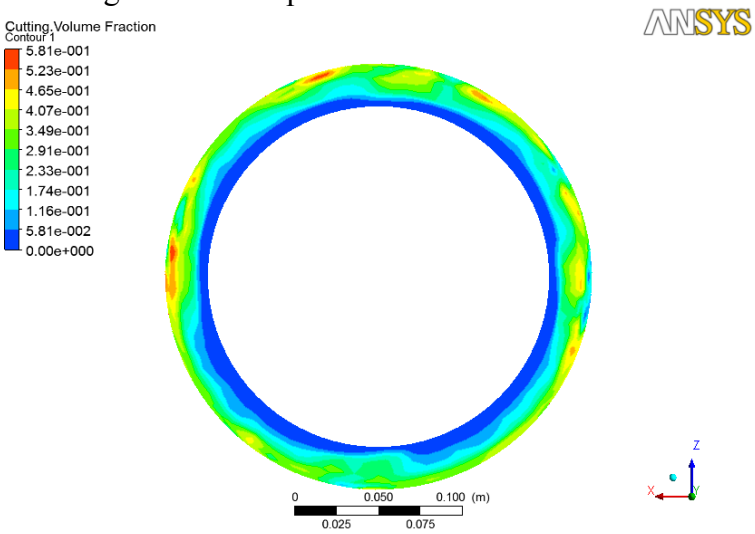

Figure 4.9 Volume Fraction of Cutting (300rpm Casing Rotational Speed)

Case 7: 200 rpm Casing Rotational Speed

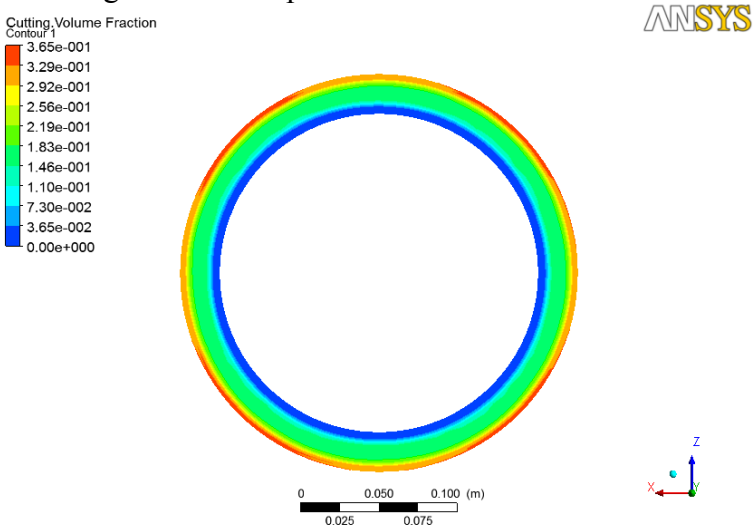

Figure 4.10 Volume Fraction of Cutting (200rpm Casing Rotational Speed)

Case 8: 100 rpm Casing Rotational Speed

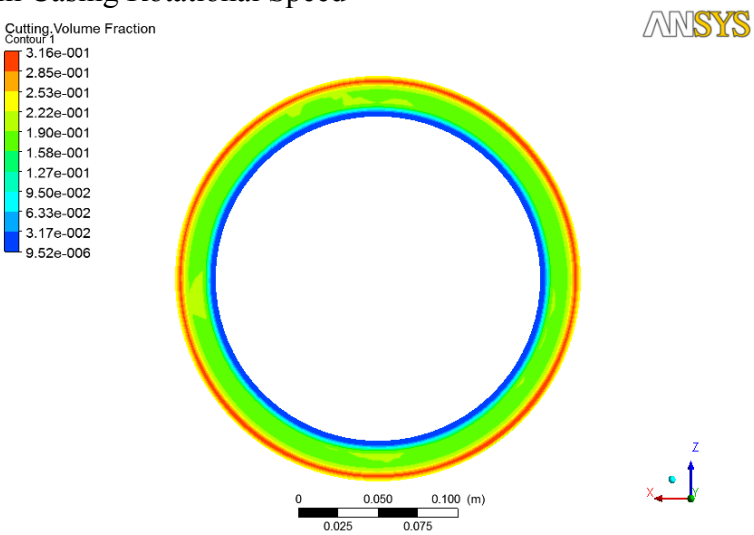

Figure 4.11 Volume Fraction of Cutting (100rpm Casing Rotational Speed)

Case 9: 60 rpm Casing Rotational Speed

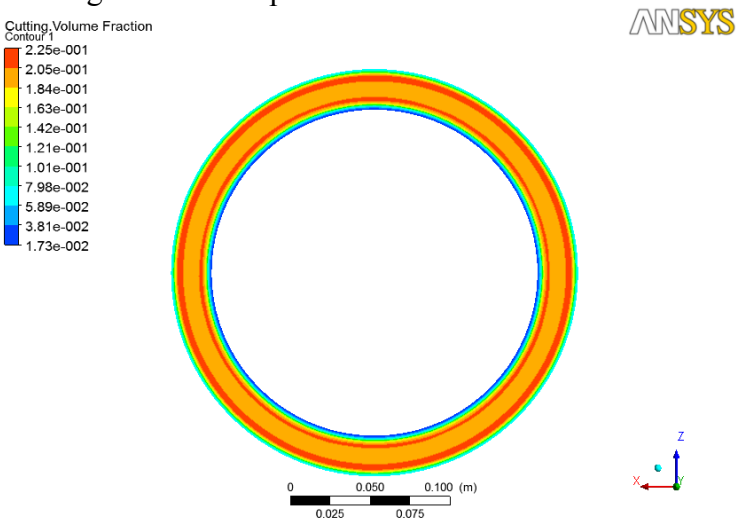

Figure 4.12 Volume Fraction of Cutting (60rpm Casing Rotational Speed)

Case 10: 0 rpm Casing Rotational Speed

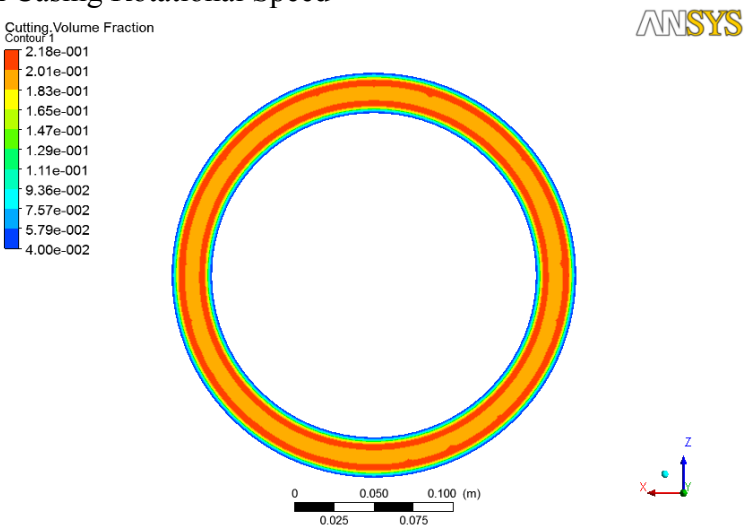

Figure 4.13 Volume Fraction of Cutting (0rpm Casing Rotational Speed)

Figure 4.9 to figure 4.13 show the contours of cutting volume fraction under different casing rotational speed conditions with same cutting particle size of 0.001m, annular velocity of 1.0 m/s and diameter ratio of 0.8. Figure 4.11 shows a nearly uniform distribution of cutting onto the wall of open hole under the condition of 100rpm casing rotational speed.

4.4.2.3 Annular Velocity: 1.5m/s

Case 11: 300 rpm Casing Rotational Speed

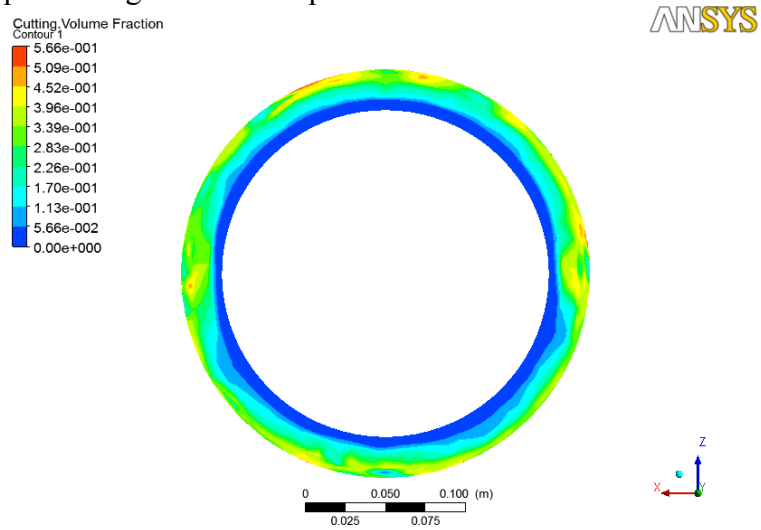

Figure 4.14 Volume Fraction of Cutting (300rpm Casing Rotational Speed)

Case 12: 200 rpm Casing Rotational Speed

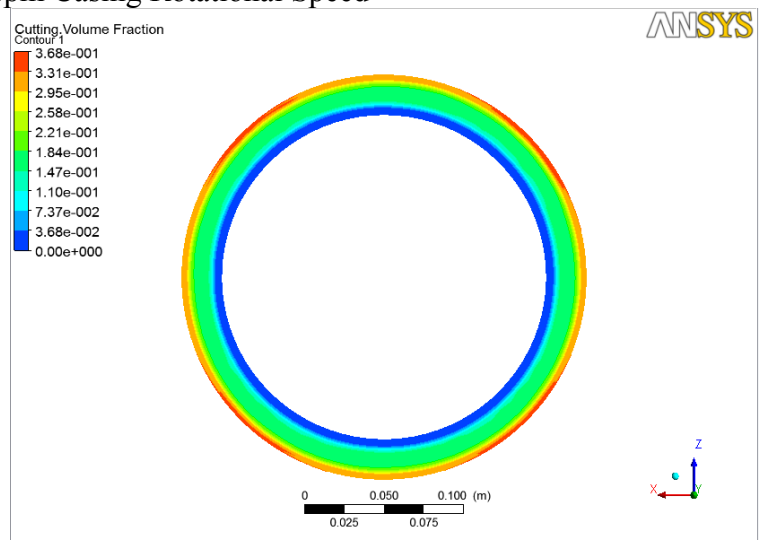

Figure 4.15 Volume Fraction of Cutting (200rpm Casing Rotational Speed)

Case 13: 100 rpm Casing Rotational Speed

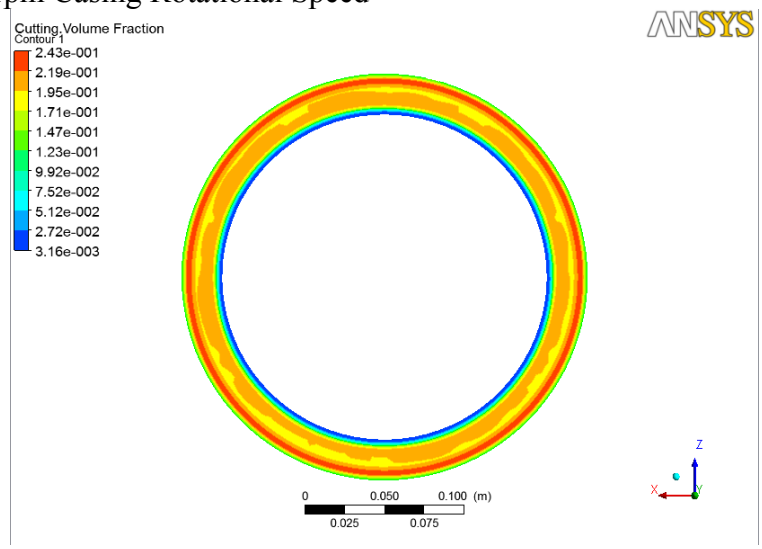

Figure 4.16 Volume Fraction of Cutting (100rpm Casing Rotational Speed)

Case 14: 60 rpm Casing Rotational Speed

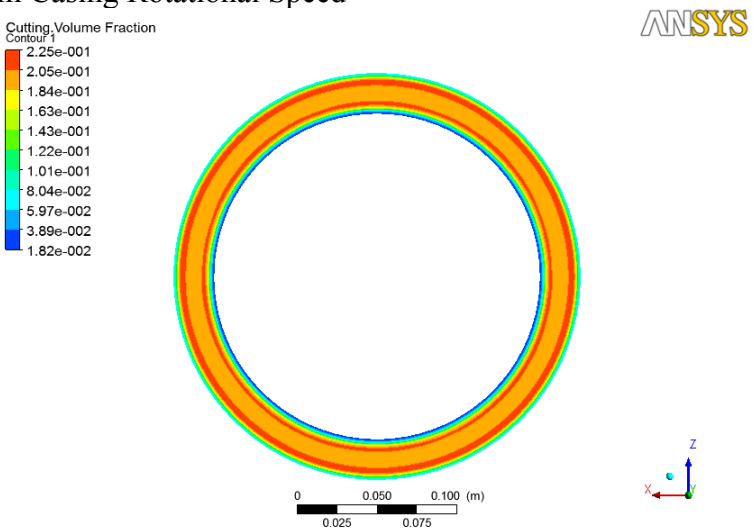

Figure 4.17 Volume Fraction of Cutting (60rpm Casing Rotational Speed)

Case 15: 0 rpm Casing Rotational Speed

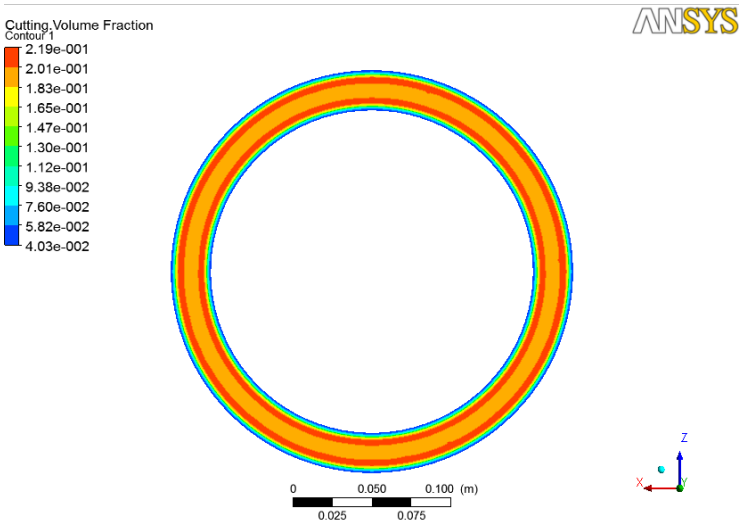

Figure 4.18 Volume Fraction of Cutting (0rpm Casing Rotational Speed)

Figure 4.14 to figure 4.18 show the contours of cutting volume fraction under different casing rotational speed conditions with same cutting particle size of 0.001m, annular velocity of 1.5 m/s and diameter ratio of 0.8. Figure 4.15 shows a nearly uniform distribution of cutting onto the wall of open hole under the condition of 200rpm casing rotational speed.

4.4.3 Concluding Remarks

4.4.3.1 0.5m/s Annular Velocity

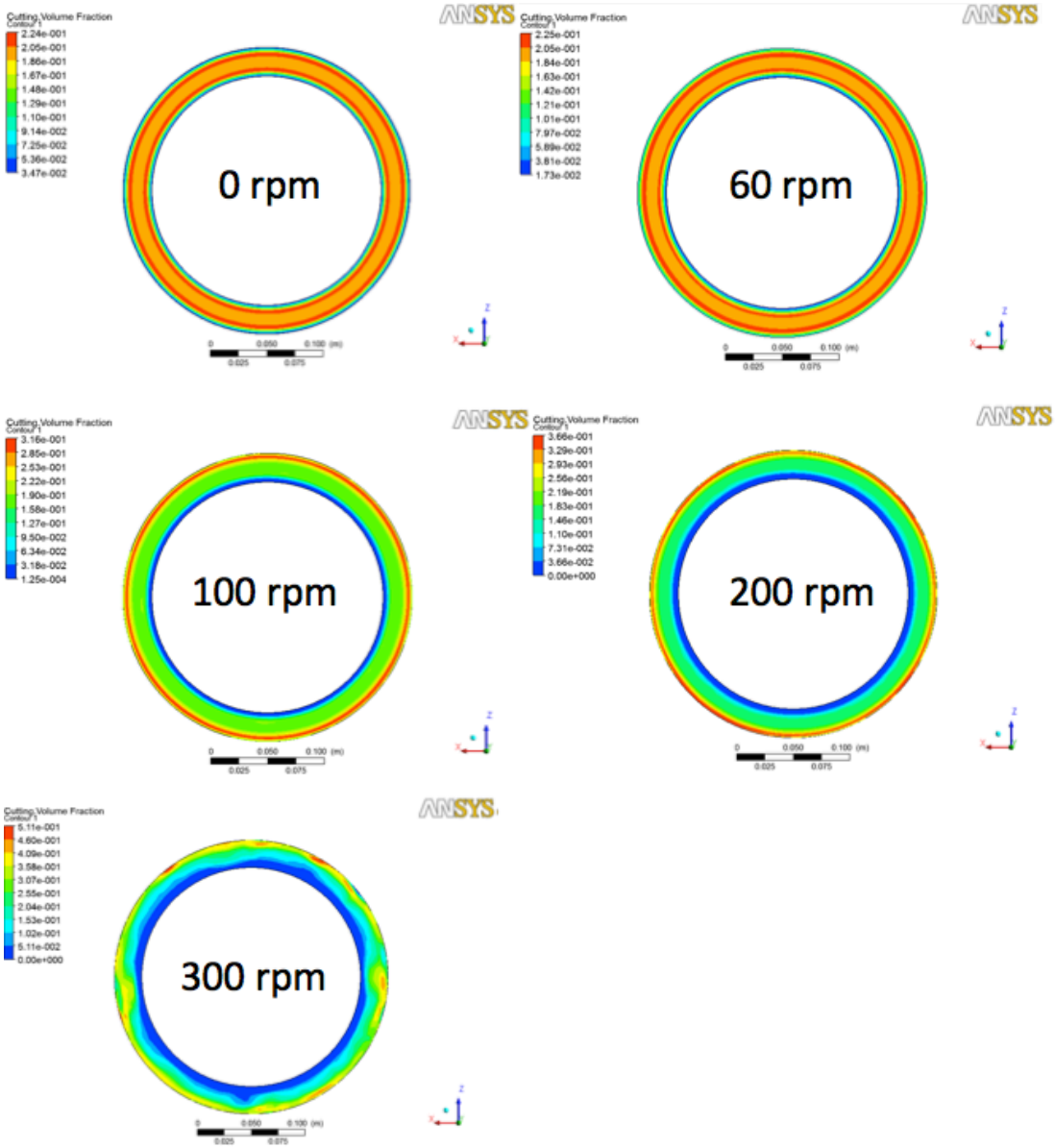

Figure 4.19 Different Casing Rotational Speed at 0.5m/s Annular Velocity

4.4.3.2 1.0m/s Annular Velocity

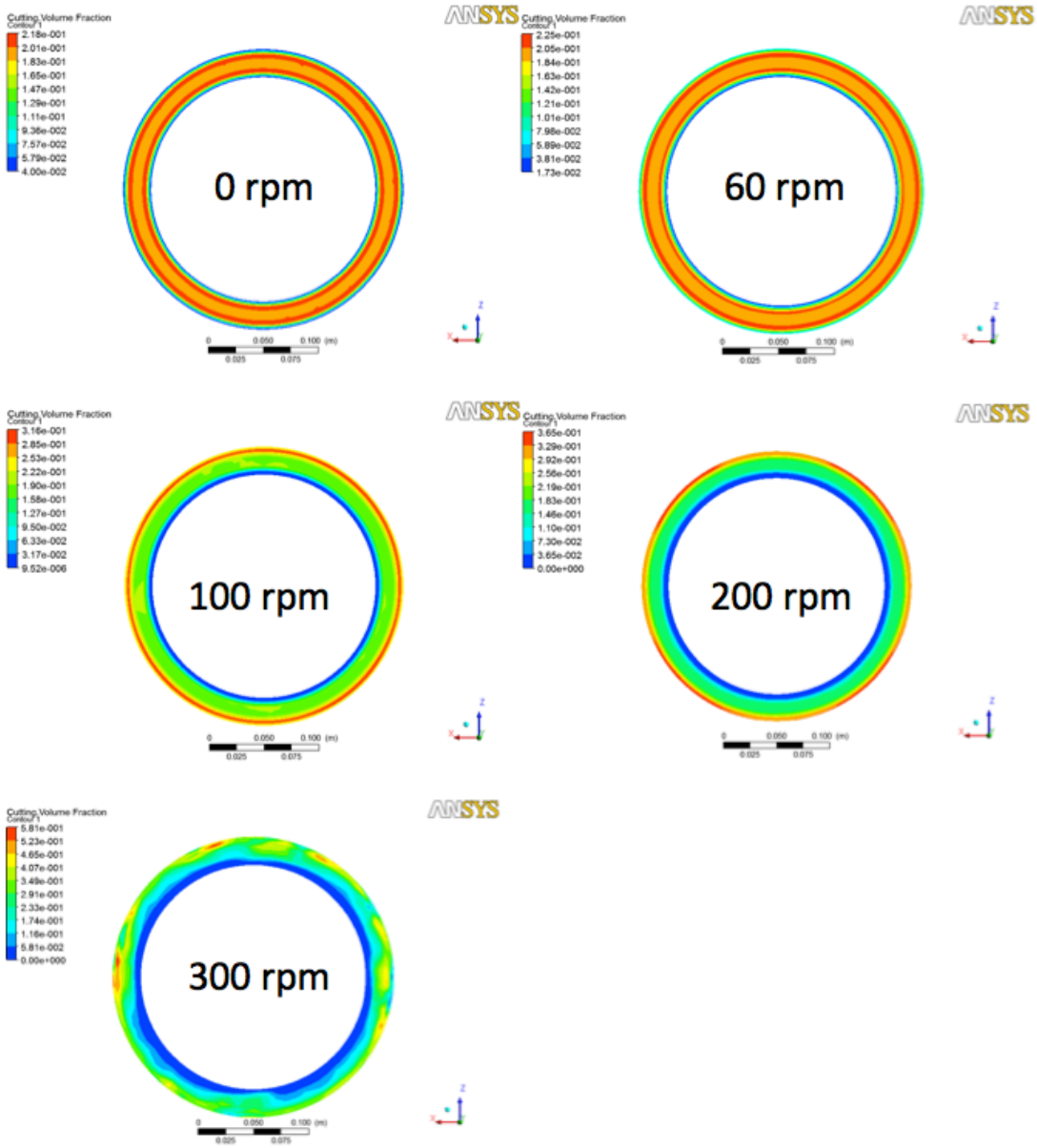

Figure 4.20 Different Casing Rotational Speed at 1.0m/s Annular Velocity

4.4.3.3 1.5m/s Annular Velocity

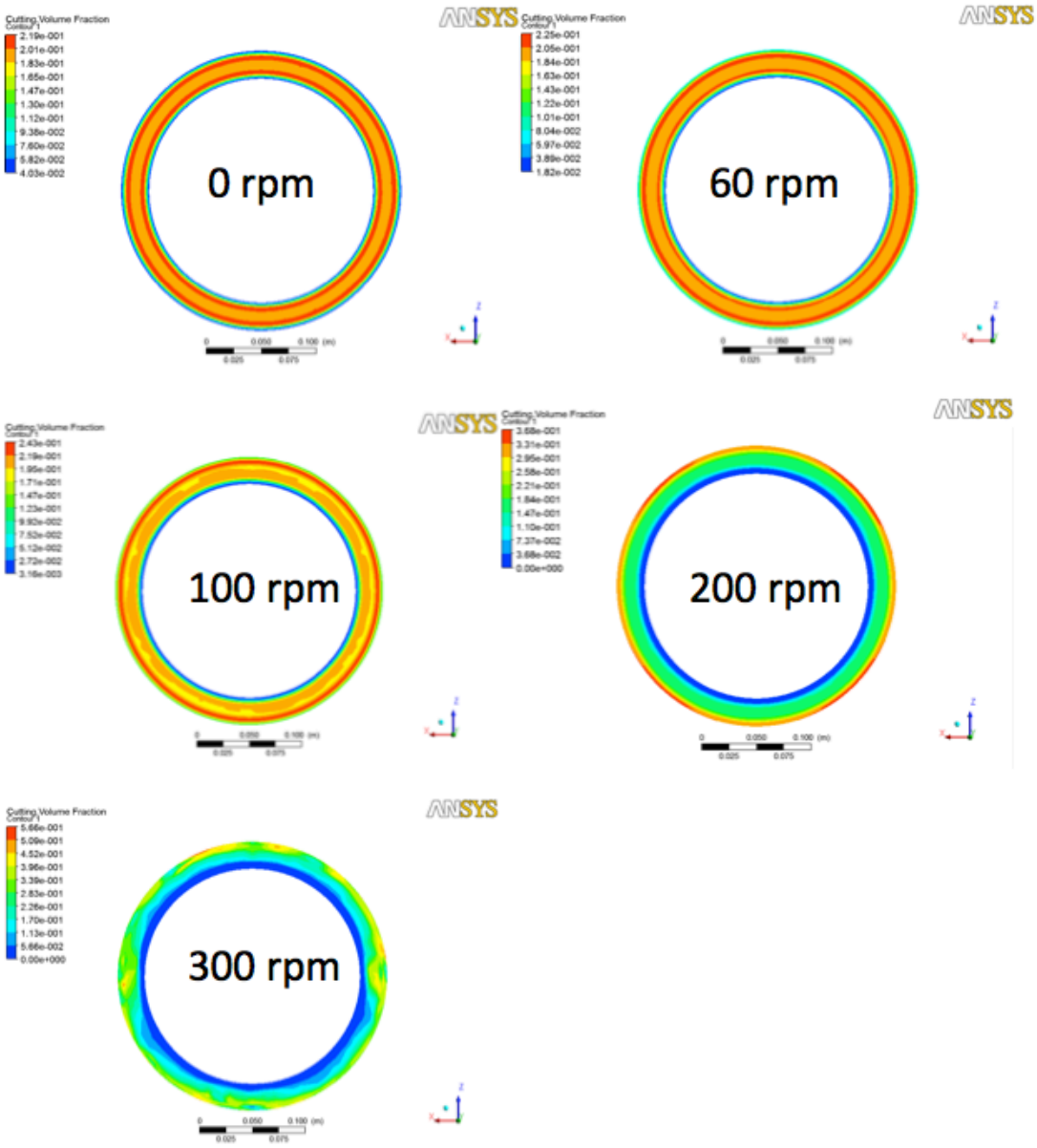

Figure 4.21 Different Casing Rotational Speed at 1.5m/s Annular Velocity

The assumed thickness of mud cake formed (x) is calculated using the equation below:

$$\text{Volume fraction of cutting} = \frac{Volume\_of\_cutting}{Total\_Volume\_of\_Annulus} \quad (4.2)$$

$$= \frac{(2\pi r_2 x) \bullet h}{\pi(r_2^2 - r_1^2) \bullet h}$$

where

r_2 = Outer radius (Open Hole); r_1 = Inner radius (Casing); x = thickness of mud cake formed

Figure 4.22 shows that study is carried out by investigating casing rotational speed on mud cake thickness varied on different annular velocities. Cutting volume fraction at the wall of open hole is higher when the casing rotational speed increases. It is thought to be that there are more cuttings are being lifted up along the annulus of wellbore and higher volume fraction of cutting is produced at the wall of open hole when casing rotational speed increases. A more uniform layer of high volume fraction of cutting is formed at the wall of open hole when casing rotational speed reaches 100rpm and 200rpm. However, 300rpm is thought to be too high for plastering effect as a non-uniform layer of high volume fraction of cutting is formed.

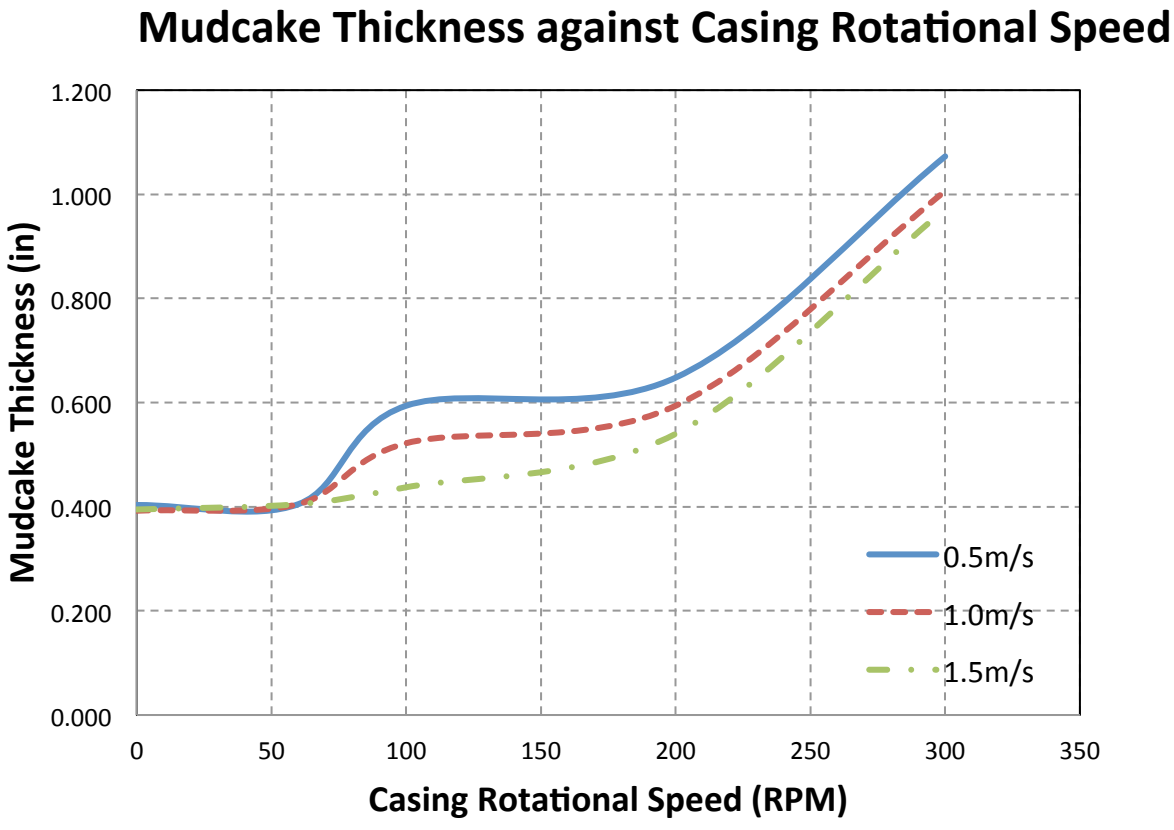

Figure 4.22 Mudcake Thickness against Casing Rotational Speed Graph

Figure 4.23 shows that study is carried out by investigating annular velocity on mud cake thickness varied on different casing rotational speeds. Cutting volume fraction at the wall of open hole decreases when the casing rotational speed increases. It is thought that there will be annular pressure loss when the flow rate is high, which will result in lower cutting volume fraction along the wall of open hole and smaller thickness of mud cake formed.

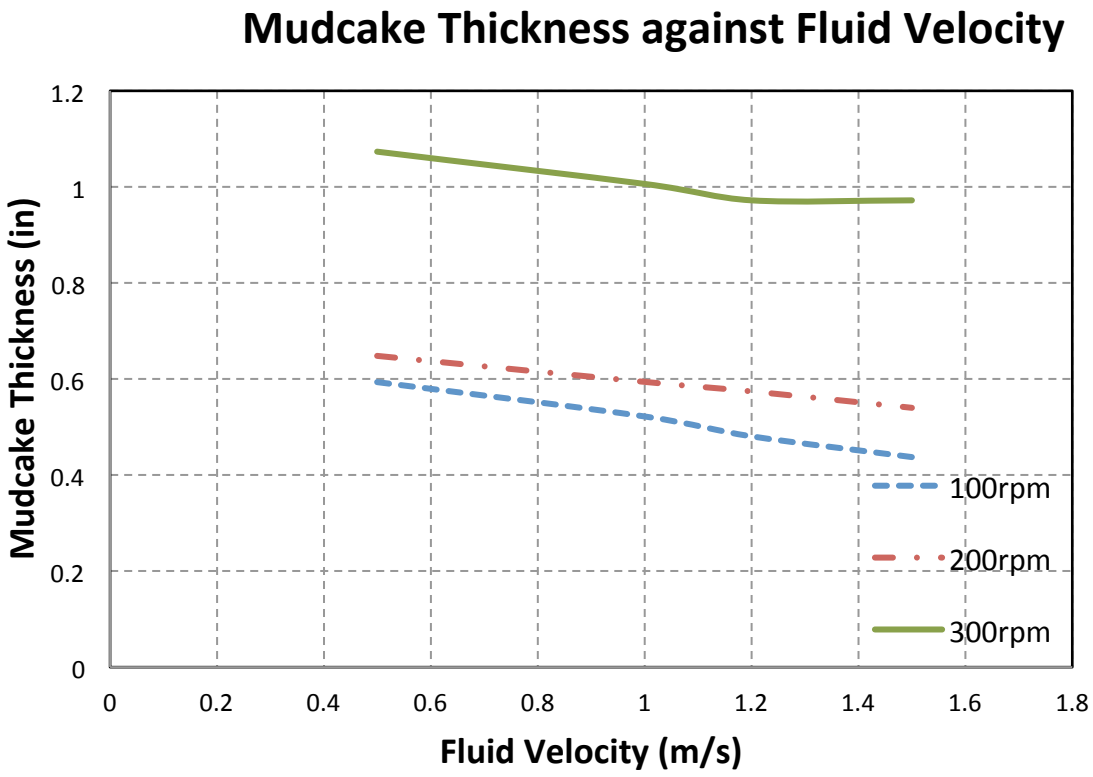

Figure 4.23 Mudcake Thickness against Annular Velocity Graph

CHAPTER 5 CONCLUSION

Plastering effect is important to CasingwhileDrilling to enhance wellbore stability. Plastering effect is modeled using ANSYS Fluent. Parameters associated with mud cake formation are studied. The casing rotational speed and annular velocity are identified as the main factors affecting the thickness of mud cake formed. Moreover, casing rotational speed will cause a significant effect to the formation of mud cake on the open hole wall. Two charts were plotted and the charts can be used to predict the mud cake thickness changes and casing rotational speed and annular velocity required for the formation of mud cake.

CHAPTER 6 REFERENCES

[1] Fontenot, K., Stickler, R. D., Molina, P., (2004) *Improved Wellbore Stability Achieved with Casing Drilling Operations Through Drilling Fluids 'Smear Effect'*. WOCWD-04-31-04. World Oil Casing While Drilling Conference, Houston.

[2] Salehi,S., Mgboji, J., Aladasani, A., Wang, S. (2013) *Numerical and Analytical Investigation of Smear Effect in Casing Drilling Technology: Implications for Enhancing Wellbore Integrity and Hole Cleaning* . SPE/IADC 163514. SPE/IADC Drilling Conference and Exhibition held in Amsterdam, The Netherlands.

[3] Alegría, L.M.C., Franco, A.T., Morales, R.E.M., Negrão, C.O.R., Martins, A.L., Waldmann, A.T.A. (2012) *Friction Factor Correlation for Viscoplastic Fluid Flows through Eccentric Elliptical Annular Pipe.* IADC/SPE 151020. IADC/SPE Asia Pacific Drilling Technology Conference and Exhibition held in Tianjin, China.

[4] Kumar, A., Samuel, R. (2013) *Analytical Model to Characterize 'Smear Effect' Observed while Drilling with Casing.* SPE/IADC 163486. SPE/IADC Drilling Conference and Exhibition held in Amsterdam, The Netherlands.

[5] Alberty, M. W., McLean, M. R. (2004) *A Physical Model for Stress Cages.* SPE 90493. SPE Annual Technical Conference and Exhibition held in Houston, Texas, U.S.A.

[6] Sarkar, A. K., Lee, J., Kasap, E. *(2000) Adverse Effects of Poor Mudcake Quality: A Supercharging and Fluid Sampling Study*. 64227-PA. SPE Reservoir Evaluation & Engineering.

[7] Fisher, K. A., Wakeman, R. J., Chiu, T. W., Meuric, O. F. J. (2000) *Numerical Modelling Of Cake Formation And Fluid Loss From Non-newtonian Muds During Drilling Using Eccentric/Concentric Drill Strings With/Without Rotation.* 0263 Trans IChemE.

[8] Moellendick, E., Karimi, M. (2011) *How Casing Drilling Improves Wellbore Stability.* AADE-11-NTCE-64**.** 2011 AADE National Technical Conference and Exhibition held at the Hilton Houston North Hotel, Houston, Texas.

[9] Mohammed, A., Okeke C. J., Okoyeagu I. A. (2012) *Current Trends and Future Development in Casing Drilling.* SSN 2224-3577 International Journal of Science and Technology.

[10] Wu, J. H., Verdín, C. T., Sepehrnoori,K., Proett, M. A. (2005) *The Influence of Water-Base Mud Properties and Petrophysical Parameters on Mudcake Growth, Filtrate Invasion, and Formation Pressure.* VOL. 46, NO. 1. Society of Petrophysicists and Well Log Analyst.

[11] Karimi, M., Moellendick, E., Holt, C. (2011) *Plastering Effect of Casing Drilling; a Qualitative Analysis of Pipe Size Contribution.* SPE 147102. SPE Annual Technical Conference and Exhibition held in Denver, Colorado, USA.

[12] Karimi, M., Petrie, S., Moellendick, E., Holt, C. (2011) *A Review of Casing Drilling Advantages to Reduce Lost Circulation, Improve Wellbore Stability, Augment Wellbore Strengthening, and Mitigate Drilling-induced Formation Damage.* SPE/IADC 148564. SPE/IADC Middle East Drilling Technology Conference and Exhibition held in Muscat, Oman.

[13] Sánchez, F., Al-Harthy, F. M. H. (2011) *Risk analysis: Casing-while-Drilling (CwD) and modeling approach*. Journal of Petroleum Science and Engineering 78.

[14] Tan, C. *Geomechanics for Sanding Prediction*. Schlumberger Kuala Lumpur Deepwater Technology Hub.

[15] Mishra, N. (2007) *Investigation of Hole Cleaning Parameters Using Computational Fluid Dynamics in Horizontal and Deviated Wells*. UMI 1451652. West Virginia University.

[16] Bilgesu, H. I., Ameri, S., Aminian, K. (2008) *Investigation of Mud Filtrate Invasion Using Computational Fluid Dynamics.*UMI 1471381. West Virginia University.

[17] Bilgesu, H.I., Ali, M.W., Aminian, K., and Ameri, S. (2002) *Computational Fluid Dynamics as a Tool to Study Cutting Transport in Wellbores*. SPE 78716. SPE Eastern Regional Meeting, Lexington, Kentucky.

[18] Civan, F. (1994) *A Multi-Phase Mud Filtrate Invasion and Wellbore Filter Cake Formation Model*. SPE 28709. SPE International Petroleum Conferences & Exhibition, Veracruz, Mexico.

[19] Proett, M., Chin W., Wu, J., and Manohar, M. (2002) *Sample Quality Prediction with Integrated Oil and Water-based Mud Invasion Modeling*. SPE 77964. SPE Asia Pacific Oil and Gas Conference and Exhibition, Melbourne, Australia.

[20] Cook, J., Growcock, F., Hodder, M., Oort, E. V. (2012) *Stabilizing the Wellbore to Prevent Lost Circulation*. Oilfield Review Winter 2011/2012-23, no. 4, Schlumberger.

[21] Kabir, M. A., Gamwo, I. K. (2011) *Filter cake formation on the vertical well at high temperature and high pressure: Computational fluid dynamics modeling and simulations*. ISSN 2141-2677. Journal of Petroleum and Gas Engineering.

[22] Metzner, A. B., Reed, J. C. (1955) *Flow of Non-Newtonian Fluids-Correlation of the Laminar, Transition, and Turbulent-Flow Regions*. Aiche Journal, 1(4), 434-440.

[23] Mokhtari, M., Ermila, M., Karimi, M. (2012) *Computational Modeling of Drilling Fluids Dynamics in Casing Drilling*. SPE 161301. SPE Eastern Regional Meeting held in Lexington, Kentucky, USA.

[24] D. Gidaspow (1994) *Multiphase Flow and Fluidization-Continuum and Kinetic Theory Descriptions*. Academic Press, San Diego.